Published in Tetrahedron 62, issue 9, 2115-2122, 2006
which should be used for any reference to this work

Dendritic liquid-crystalline fullerene–ferrocene dyads

Stéphane Campidelli,[a] Laura Pérez,[b] Julián Rodríguez-López,[b] Joaquín Barberá,[c,*] Fernando Langa[b,*] and Robert Deschenaux[a,*]

[a]*Institut de Chimie, Université de Neuchâtel, Avenue de Bellevaux 51, Case Postale 2, 2007 Neuchâtel, Switzerland*
[b]*Facultad de Ciencias del Medio Ambiente, Universidad de Castilla-La Mancha, 45071 Toledo, Spain*
[c]*Química Orgánica, Facultad de Ciencias-Instituto de Ciencia de Materiales de Aragón, Universidad de Zaragoza-CSIC, 50009 Zaragoza, Spain*

Dedicated to Prof. David I. Schuster on the occasion of his 70th birthday

Abstract—First- and second-generation ferrocene-based dendrimers, fullerene and a second-generation liquid-crystalline poly(arylester) dendrimer carrying four cyanobiphenyl units were assembled to elaborate polyfunctional materials displaying mesomorphic and electronic properties. The targeted compounds gave rise to enantiotropic smectic A phases and organized into bilayer structures within the smectic layers. Cyclic voltammetry investigations revealed oxidation and reduction processes in agreement with the presence of both ferrocene and fullerene units. Finally, strong quenching of the fluorescence was obtained for the fullerene–ferrocene dyads suggesting efficient elecron transfer from the ferrocene-based dendrimer to fullerene.

1. Introduction

A rich variety of electron donors, including TTF,[1] conjugated oligomers,[2] porphyrins[3] and ferrocenes,[4] were associated to [60]fullerene (C_{60}) in order to generate efficient intramolecular electron transfer. The design of photoactive [60]fullerene-based materials for applications in photovoltaic[2a,b,5] and organic light emitting diode[6] technologies strongly motivated synthetic efforts in this research area. Furthermore, recent developments in liquid crystal technology demonstrated that columnar phases, in which high-hole mobility along the columns was observed, were found to be a suitable medium for photovoltaic applications.[7] Therefore, functionalized liquid-crystalline fullerenes are promising materials for applications in electronic and optical nanotechnologies as they combine the unique properties of C_{60} with the characteristics of liquid crystals.

We designed liquid-crystalline ferrocene–fullerene dyads in which photoinduced electron transfer was observed.[8] Such materials could act as photoactive supramolecular switches providing the lifetime of the charge separated state is long enough. The switching mechanism would be based on the different intermolecular interactions generated by either the neutral ferrocene species (light off) or the cationic ferrocenium species (light on): we were able to obtain either smectic A or rectangular columnar phases from the oxidation of non-mesomorphic ferrocene derivatives.[9] This behavior could be extended to liquid-crystalline ferrocene–fullerene dyads.

To further explore the properties of liquid-crystalline dyads based on ferrocene and C_{60}, we decided to use a dendritic-like ferrocene architecture as a source of electrons. Ferrocene-based dendrimers display remarkable electrochemical properties and have been used for the construction of batteries[10] and sensors.[11] The association of a ferrocene-containing dendrimer and C_{60} within a liquid-crystalline structure could lead to polyfunctional materials displaying interesting mesomorphic, photophysical and electrochemical properties.

We report, herein, the synthesis, liquid-crystalline properties, supramolecular organization, electrochemical and photophysical behavior of fullerene–ferrocene dyads **1** and **2** containing two and four ferrocene units, respectively. A second-generation poly(arylester) dendrimer functionalized with cyanobipenyl units was used as liquid-crystalline promoter (Chart 1).

2. Results and discussion

2.1. Synthesis

The synthetic procedure used for the preparation of **1** and **2** is shown in Scheme 1. Fulleropyrrolidines **5** and **6** were

Keywords: Ferrocene; Fullerene; Supramolecular organization.
* Corresponding authors. Fax: +34 925268840 (F.L.); e-mail addresses: jbarbera@unizar.es; fernando.lpuente@uclm.es; robert.deschenaux@unine.ch

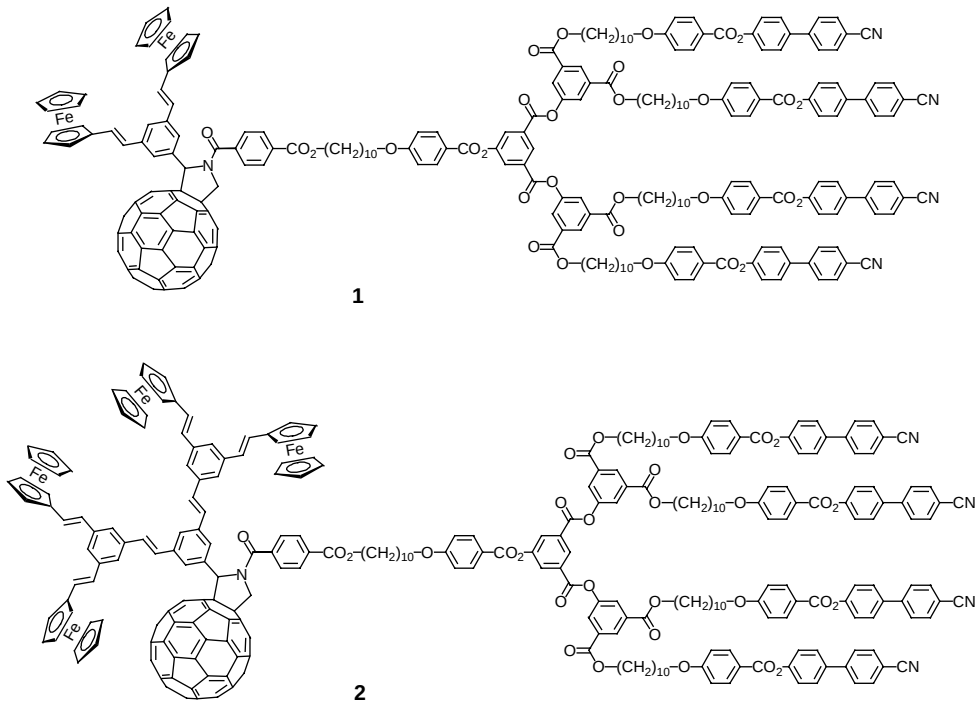

Chart 1.

prepared by 1,3-dipolar cycloaddition of C_{60} with the azomethine ylide[12] generated in situ from aldehyde functionalized dendrons **3** or **4** and glycine in refluxing chlorobenzene. Monoadducts **5** and **6** were obtained in 32 and 30% yield, respectively, after purification by column chromatography (silica gel, toluene/hexane 7:3). The synthesis of targeted compounds **1** and **2** involved reaction of acid **7a** with thionyl chloride in CH_2Cl_2 to prepare the corresponding acid chloride **7b** followed by condensation of the latter with **5** or **6** in refluxing CH_2Cl_2 (quantitative yields), and purification by column chromatography (silica gel, toluene/hexane 4:1).

All new compounds were characterized by ^1H and ^{13}C NMR, FT-IR and MALDI-TOF mass spectrometry. The analytical data were in agreement with the structures. High resolution ^1H NMR spectra of *NH*-fulleropyrrolidines **5** and **6** showed all the expected signals. The ferrocene protons are shown between 4 and 5 ppm as two groups of signals; the typical pyrrolidine protons [two doublets (AB system) and one singlet] appeared in the 4–5 ppm range. The *E*-configuration of the vinyl hydrogens in the ferrocene-based dendrimer ($J = 16$–17 Hz) is observed. In target structures **1** and **2**, the signals described for precursors **5** and **6** remain, appearing together with the typical signature of mesogenic dendrimers.[8,9] MALDI-TOF mass spectrometry showed the M+1 molecular ion peak for **1** and **2** and the M molecular ion peak for **5** and **6**. UV–vis spectra revealed the typical dihydrofullerene absorption band at around 430 nm. The synthesis of **3**, **4** and **7a** will be reported separately with other dendritic materials.

2.2. Liquid-crystalline properties

The thermal and liquid-crystalline properties of **1**, **2** and **7a** were investigated by polarized optical microscopy (POM) and differential scanning calorimetry (DSC). The mesomorphic behavior of **1** and **2** was also analyzed by X-ray diffraction (XRD). The phase transition temperatures and enthalpies are reported in Table 1.

Compounds **1**, **2** and **7a** gave rise to smectic A phases, which were identified by POM from the observation of typical focal-conic and homeotropic textures. Fullerene derivatives **1** and **2** showed a lower clearing point than liquid-crystalline dendrimer **7a**. This behavior is in agreement with results obtained for other fullerene-containing liquid crystals,[13] and is attributed to the presence of bulky ferrocene and C_{60} units.

The X-ray diffraction patterns recorded at room temperature from as-obtained samples of **1** and **2** were consistent with the formation of smectic A phases. They contained a set of two equally-spaced maxima at low angles, which are typical of lamellar systems. These maxima were sharp and corresponded to the first and second order reflections. By applying Bragg's law to these maxima, layer spacings of 93 and 105 Å were obtained for **1** and **2**, respectively. No reflections were found at middle and high angles, except for a diffuse scattering halo, which was characteristic of the liquid-like packing inside the smectic layers. This halo, which corresponded to an average distance of about 4.5 Å for **1** and 4.3 Å for **2**, is usually found in X-ray diffractograms of liquid crystal phases and confirms the mesomorphic nature of the room temperature phases displayed by **1** and **2**.

The diffraction patterns did not change after thermal treatment of the samples, which were heated above the clearing point and then cooled to room temperature. In the case of **1**, experiments were carried out at different temperatures between the glass transition temperature and

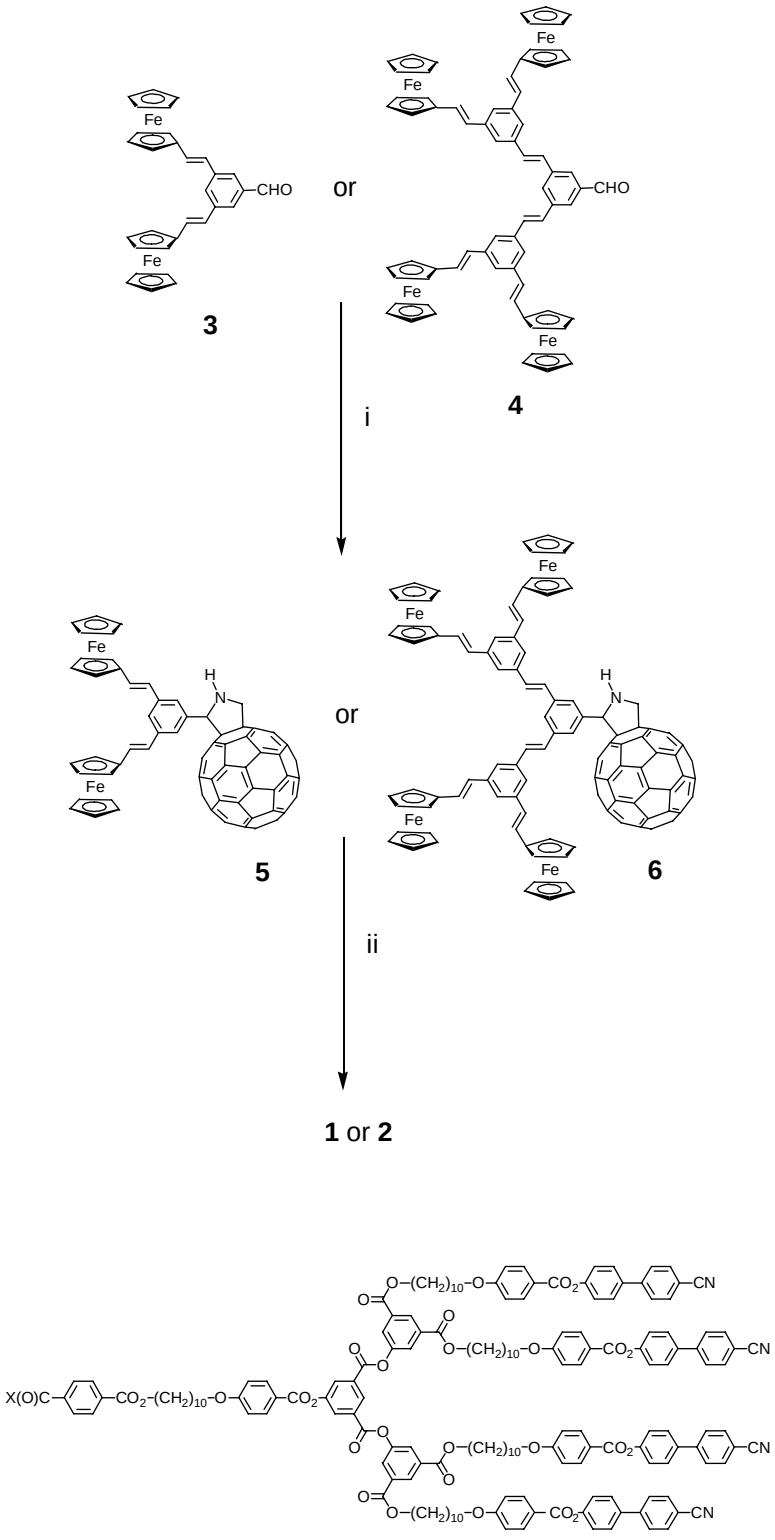

Scheme 1. Reagents and conditions: (i) C_{60}, glycine, chlorobenzene, reflux, 8 h, yield: 32% for **5**, 30% for **6**; (ii) **7a**, thionyl chloride, CH_2Cl_2, reflux, 7 h, then **5** or **6**, CH_2Cl_2, pyridine, room temperature, 2 h, quantitative yields.

the clearing point. These experiments confirmed that the mesophase was smectic A in nature within the mesomorphic domain. No differences were observed between the X-ray patterns recorded below and above the glass transition. This result meant that the room temperature phase was a frozen smectic A phase with the same structure as the high-temperature liquid crystal phase but lacking fluidity. When the possible temperature dependence of the layer thickness was tested, the measured values were found to be constant within the accuracy of the measurements. Thus, it can be

Table 1. Phase-transition temperatures and enthalpy changes of **1**, **2** and **7a**[a]

Compound	T_g (°C)[b]	$S_A \rightarrow I$ (°C)	ΔH (kJ/mol)
1	47	171[c]	7.3
2	34	168[c]	13.3
7a	45	203[d]	18.6

[a] T_g = glass transition temperature, S_A = smectic A phase, I = isotropic liquid.
[b] Determined during the first cooling run.
[c] Determined as the maximum of the peak obtained during the second heating run.
[d] Determined as the onset of the peak obtained during the second heating run.

concluded that the temperature had no significant effect on the molecular conformations or on the extent of interdigitation (see below).

2.3. Supramolecular organization

The molecular lengths (L) of **1** and **2**, in their extended conformation, were estimated by means of HyperChem software, and were estimated to be 70 Å for **1** and 77 Å for **2**. The d/L ratio of 1.33 for **1** and of 1.36 for **2** revealed that **1** and **2** organized into a bilayer smectic structure with alternate sublayers of cyano-biphenyl units, fullerene units and ferrocene units (Fig. 1). Such a supramolecular organization is driven by steric constraints resulting from the difference of the cross-sectional area of C_{60} (90–100 $Å^2$), ferrocene (45 $Å^2$) and the four mesogenic groups (22–25 $Å^2$ per mesogenic unit). For **1**, there is a good adequacy of the cross-sectional areas of each part of the molecule (four mesogenic units, one C_{60} unit and two ferrocene units), and an average value of about 100 $Å^2$ is obtained. In **2**, there are four ferrocene units, leading to a cross-sectional area of about 180 $Å^2$, that is, twice as much than in **1**. For **2**, the difference in cross-sectional areas is, most likely, compensated by a different orientation of the poly(arylester) dendrimer, so efficient space filling is obtained. Finally, interdigitation of the cyanobiphenyl units from one layer to the adjacent one should contribute to the stabilization of the layers.

2.4. Electrochemistry

The determination of the redox potentials in donor–acceptor systems is important to evaluate the energetics of electron transfer reactions. We performed a systematic study to evaluate the redox properties of **1**, **2**, **5**, **6**, **7a**, and of ferrocene and C_{60} used for comparative purposes, using cyclic (CV) and Osteryoung square wave voltammetry (OSWV) (Table 2, Fig. 2). As illustrated in Figure 2 for **1**, the CV curves of **1**, **2**, **5** and **6** showed that they were electrochemically active in both anodic and cathodic sweep directions between +1.0 and −2.5 V. In the cathodic scan, three reversible reduction waves were observed and presumably, fullerene centred, but shifted to more negative values than those observed for C_{60} because of the saturation of one double bond of the C_{60} cage.[12] An additional non-reversible reduction wave was observed for **1** and **2** at

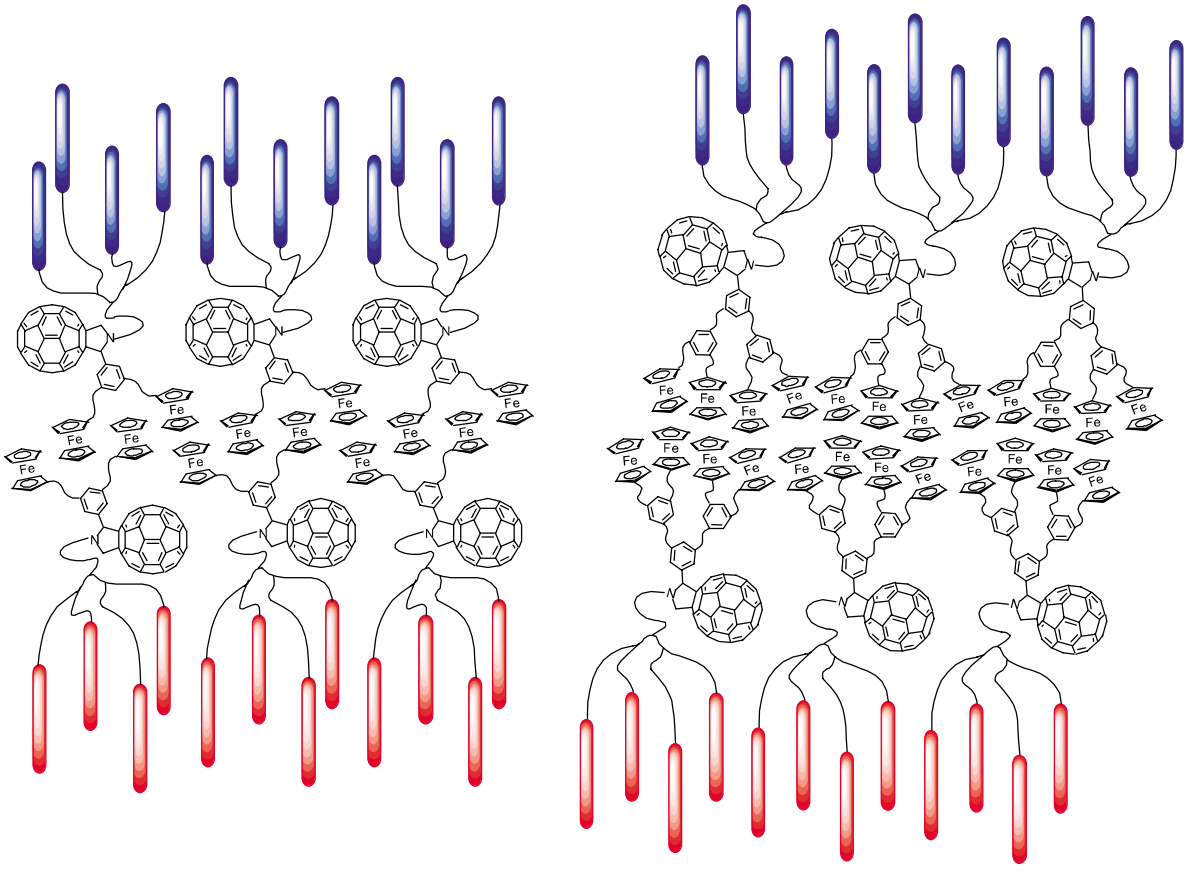

Figure 1. Postulated supramolecular organization of **1** (left) and **2** (right) within the smectic A phase.

Table 2. Osteryoung square wave voltammetry (OSWV) data in *o*-dichlorobenzene–acetonitrile (4/1)[a]

	E^1_{red} (V)	E^2_{red} (V)	E^3_{red} (V)	E^4_{red} (V)	E^1_{ox} (V)
1	−1.02	−1.41	−1.96	−2.11	0.01
2	−1.01	−1.40	−1.96	−2.08	−0.03
5	−1.10	−1.49	−2.00		0.03
6	−1.04	−1.44	−1.98		
7a				−2.08	
C_{60}	−0.99	−1.38	−1.85		
Ferrocene					0.04

[a] V versus $Ag/AgNO_3$; glassy carbon electrode as the working electrode; 0.1 M TBAP; scan rate = 100 mV s^{-1}; concentration: 1.4×10^{-3} M.

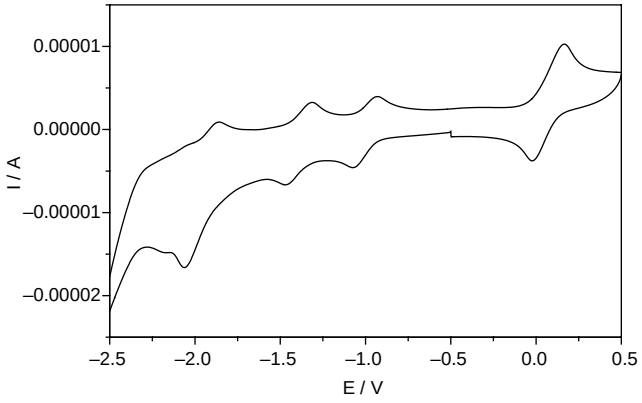

Figure 2. Cyclic voltammogram of **1**.

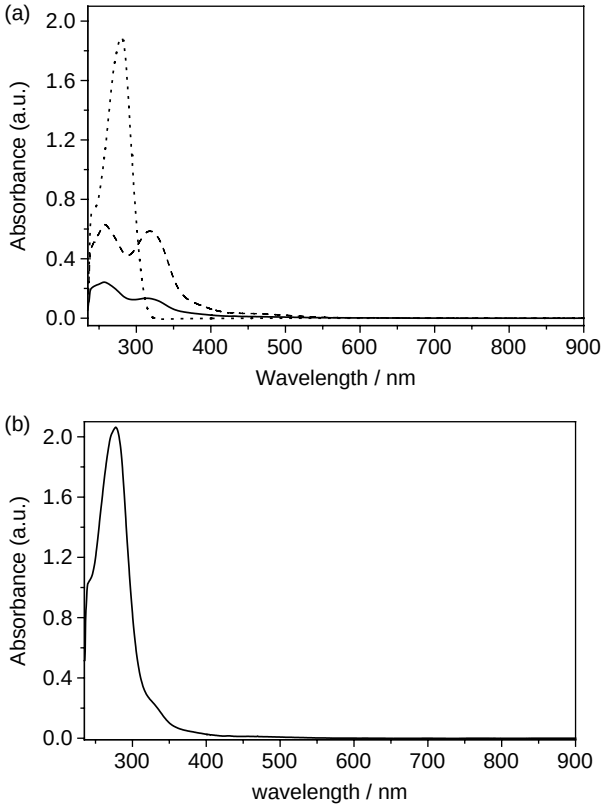

Figure 3. (a) Absorption spectra in chloroform (10^{-5} M) of **5** (solid line), **6** (dashed line) and **7a** (dotted line). (b) Absorption spectra in chloroform (10^{-5} M) of **1**.

around −2.10 V, which was assigned to the reduction of the mesogenic dendrimer by comparison with the reduction wave observed for **7a**. In the anodic scan, the observed oxidation process is ferrocene-based because no oxidation can be observed for **7a** in this region. The experimentally determined HOMO–LUMO gap (ΔE) is lower (0.98 eV) for the second-generation ferrocene dendrimer derivative **2** compared with that of **1** (1.03 eV). The same trend is found for precursor *NH*-fulleropyrrolidine **6** (1.04 eV) with respect to **5** (1.13 eV).

2.5. Photophysical studies

The absorption spectra of **5** and **6** were measured in $CHCl_3$ (Fig. 3a) and display λ_{max} values at 257 nm (log ε = 4.38) and 313 nm (log ε = 4.13) for **5** and 258 nm (log ε = 4.80) and 318 nm (log ε = 4.77) for **6** indicating that conjugation is not extended by *meta*-substitution. Consequently, **5** and **6** behave as an assembly of two and four vinylferrocene moieties sharing a phenyl ring. Both fullerene–ferrocene dendrimers show the typical small band for [6,6]-bridged fullerene derivatives at 431 nm. On the other hand, **7a** show only one λ_{max} value at 279 nm (log ε = 5.28). Absorption spectra of **1** and **2** in $CHCl_3$ are dominated by the mesogenic moiety, showing maxima at 279 nm, and were essentially the sum of the spectra of the corresponding components (**5** or **6**) and **7a** (Fig. 3b). Weak absorptions typical for fulleropyrrolidines were observed around 430 and 700 nm, respectively (not shown).

The fluorescence of functionalized fullerene derivatives is a sensitive parameter, which can be used to probe intramolecular transfer processes in donor–acceptor systems.[14] Emission spectra of *N*-methylfulleropyrrolidine, used as reference, show maxima around 710 nm,[3b,15] independently of the polarity of solvent. We studied the room temperature fluorescence spectra of **1**, **2**, **5** and **6** using *N*-methylfulleropyrrolidine as reference, in toluene and benzonitrile with excitation at 430 nm, wavelength where only the fullerene cage is excited.[16] In toluene, the fluorescence observed at 714 nm for *N*-methylfulleropyrrolidine was almost totally quenched in **5** and **6** (only a weak emission at 704 nm is observed) independently of the generation of the dendrimer (Fig. 4a). When the most polar benzonitrile solvent was used, the fluorescence was totally quenched. These findings suggested the occurrence of an efficient electron transfer process from the ferrocene-based dendrimer to C_{60}. Efficient electron transfer processes in fullerene–ferrocene dyads were previously observed.[4a,17] Similar behavior was observed for **1** and **2** (Fig. 4b), with respect to the properties observed for **5** and **6**, indicating that the newly incorporated mesogenic dendrimer did not influence the photophysical behavior of the studied materials.

3. Conclusion

We have designed a novel family of liquid-crystalline fullerene–ferrocene dyads by assembling a first- or second-generation ferrocene-based dendrimer, a second-generation mesomorphic poly(arylester) dendrimer carrying

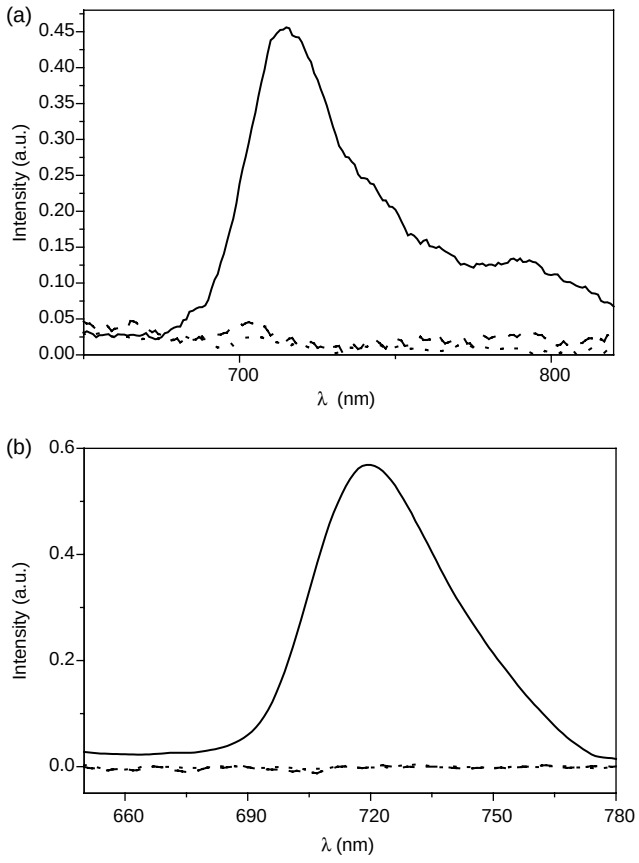

Figure 4. (a) Steady-state fluorescence ($\lambda_{exc}=430$ nm) of **5** (dashed line), **6** (dotted line) and *N*-methylpyrrolidino[60]fullerene (solid line) measured in toluene. (b) Steady-state fluorescence ($\lambda_{exc}=430$ nm) of **1** (dashed line), **2** (dotted line) and *N*-methylpyrrolidino[60]fullerene (solid line) measured in benzonitrile.

cyanobiphenyl units and fullerene. The materials dispayed smectic A phases, and the supramolecular organization was governed by steric constraints. The electrochemical behavior was in agreement with the redox-activity of the building-blocks. Steady-state emission spectra showed that the fluorescence was totally quenched, suggesting the existence of an efficient electron transfer process from the ferrocene dendrimer to C_{60}. Therefore, the use of ferrocene-based dendrimers as electron donor moieties could be appealing to elaborate supramolecular switches based on fullerene and ferrocene.

4. Experimental

4.1. General procedures

All the cycloaddition reactions were performed under argon. C_{60} was purchased from MER Corporation (Tucson, AZ, USA) and the commercial starting materials were purchased from ACROS. Cycloaddition reactions were monitored by TLC using Merck silica gel 60-F_{254}. ^{1}H and ^{13}C NMR spectra were recorded on a Varian Mercury 200 apparatus. UV–vis absorption spectra were obtained on a Shimatzu spectrophotometer. FT-IR spectra were recorded on a Nicolet AVATAR 370 spectrophotometer on KBr discs. Transition temperatures (onset point) and enthalpies were determined with a differential scanning Mettler DSC 822 calorimeter, under N_2/He, at a rate of 10 °C/min. Optical studies were conducted using a Zeiss-Axioscope polarizing microscope equipped with a Linkam-THMS-600 variable-temperature stage, under N_2. The XRD patterns were obtained with a pinhole camera (Anton-Paar) operating with a point-focussed Ni-filtered Cu Kα beam. The samples were held in Lindemann glass capillaries (1 mm diameter) and heated, when necessary, with a variable-temperature oven. The patterns were collected on flat photographic films. The capillary axis and the film are perpendicular to the X-ray beam. Spacings were obtained via Bragg's law. MALDI-TOF mass spectra were obtained on a Voyager DE-STR from Applied Biosystems, using ditranol as a matrix. Cyclic voltammetry measurements were obtained using a Versastat PAR EG and G potentiostat with analytical electrochemical software (Mod. 250). The measurements were made in a double-walled cell (Metrohm EA 876-20). A glassy carbon working electrode (Metrohm 6.0804.010) was used after being polished with alumina (0.3 μ) for 1 min, and platinum wire was used as counter electrode. An $Ag/AgNO_3$ electrode, used as a reference electrode, was separated from the solution by a solution of tetrabutylammonium perchlorate, which was used as the supporting electrolyte in toluene/acetonitrile 4:1. The samples were purged with argon prior to measurement.

4.1.1. Synthesis of 5. A mixture of C_{60} (122.4 mg, 0.17 mmol), **3** (20 mg, 0.038 mmol) and glycine (14.3 mg, 0.19 mmol) was heated under reflux for 8 h in degassed anhydrous chlorobenzene (30 mL) under inert atmosphere. After removal of the solvents, the residue was purified over silica gel (toluene/hexane 7:3). The product was centrifuged with CH_3OH and *n*-pentane to give **5** (32%) as a dark brown solid. ^{1}H NMR (200 MHz, $CDCl_3$): δ 4.14 (s, 10H, C_5H_5), 4.31 (t, 4H, $J=1.8$ Hz, HCp), 4.50 (t, 4H, $J=1.8$ Hz, HCp), 4.87 (A of AB_q, 1H, $J=10.2$ Hz, $H_2C_{pyrrol.}$), 5.17 (B of AB_q, 1H, $J=10.2$ Hz, $H_2C_{pyrrol.}$), 5.84 (s, 1H, $HC_{pyrrol.}$), 6.74 (A of AB_q, 2H, $J=16.2$ Hz, CH═), 6.95 (B of AB_q, 2H, $J=16.2$ Hz, CH═), 7.44 (s, 1H, $H_{arom.}$), 7.75 (s, 2H, $H_{arom.}$). ^{13}C NMR (125 MHz, $CDCl_3$): δ 155.95, 153.77, 153.47, 152.78, 147.04, 146.74, 146.34, 146.22, 146.01, 145.81, 145.62, 145.41, 145.32, 145.08, 144.83, 144.52, 144.27, 143.10, 142.91, 142.62, 142.40, 142.22, 142.07, 141.94, 141.70, 141.64, 141.50, 140.15, 140.11, 139.79, 139.56, 138.49, 137.02, 136.49, 136.35, 136.04, 135.81, 135.54, 128.22, 128.13, 127.82, 125.54, 123.77, 123.61, 123.37, 122.94, 82.93, 77.59, 77.08, 69.28, 69.20, 66.98, 61.72, 53.37. UV–vis λ_{max} (nm) (log ε, $CHCl_3$): 257 (4.38), 313 (4.13), 431 (3.14). IR (KBr) ν (cm^{-1}) 1510, 835, 538. MALDI-MS, *m/e* 1259.1 (M).

4.1.2. Synthesis of 6. Prepared as **5** from **4** (44 mg, 0.038 mmol). Yield: 30%. ^{1}H NMR (200 MHz, $CDCl_3$): δ 4.17 (s, 20H, C_5H_5), 4.33 (t, 8H, $J=1.6$ Hz, HCp), 4.51 (t, 8H, $J=1.8$ Hz, HCp), 4.92 (A of AB_q, 1H, $J=10.4$ Hz, $H_2C_{pyrrol.}$), 5.16 (B of AB_q, 1H, $J=10.4$ Hz, $H_2C_{pyrrol.}$), 5.86 (s, 1H, $HC_{pyrrol.}$), 6.75 (A of AB_q, 4H, $J=16.2$ Hz, CH═), 6.98 (B of AB_q, 4H, $J=16.0$ Hz, CH═), 7.24 (s broad, 4H, CH═), 7.39 (s, 2H, $H_{arom.}$), 7.48 (s broad, 4H, $H_{arom.}$), 7.74 (s, 1H, $H_{arom.}$), 7.90 (s, 2H, $H_{arom.}$). ^{13}C NMR (50 MHz, $CDCl_3$): δ 156.08, 153.88, 153.30, 150.78,

150.60, 150.29, 149.80, 149.40, 148.40, 148.24, 147.60, 147.47, 147.24, 146.70, 146.33, 146.29, 145.72, 145.52, 145.32, 145.06, 144.45, 143.09, 142.87, 142.42, 142.27, 141.93, 140.50, 138.93, 138.79, 138.47, 138.38, 137.48, 135.85, 134.12, 133.96, 133.74, 133.53, 133.31, 130.77, 130.02, 129.64, 127.95, 127.74, 127.71, 125.99, 123.57, 122.73, 83.50, 81.36, 73.04, 69.55, 69.45, 69.44, 67.18. UV–vis λ_{max} (nm) (log ε, $CHCl_3$): 258 (4.80), 318 (4.77), 431 (3.57). IR (KBr) ν (cm^{-1}) 1531, 625, 528. MALDI-MS, *m/e* 1883.2 (M).

4.1.3. Synthesis of 1. A mixture of **7a** (100 mg, 0.036 mmol) and thionyl chloride (0.1 mL, 1.3 mmol) was heated under reflux for 7 h in anhydrous CH_2Cl_2. The solvent was evaporated under reduced pressure and added to a solution of **5** (20 mg, 0.016 mmol) in 25 mL of CH_2Cl_2 and anhydrous pyridine (1.5 mg, 0.02 mmol). The mixture was stirred at room temperature for 2 h. After evaporation of the solvent under reduced pressure, the residue was purified by column chromatography (toluene/hexane 4:1). A further purification by centrifugation with CH_3OH afforded **1** in quantitative yield as a dark brown solid. ^{1}H NMR (200 MHz, $CDCl_3$): δ 1.24–1.70 (m broad, 60H, $H_{aliph.}$), 1.72–1.92 (m broad, 20H, $5\times CO_2CH_2CH_2+5\times CH_2CH_2O$), 4.03 (t, 10H, $J=6.4$ Hz, CH_2O), 4.14 (s, 10H, C_5H_5), 4.36 (m, 14H, $4\times HCp+5\times CO_2CH_2$), 4.50 (t, 4H, $J=1.8$ Hz, HCp), 5.80 (AB_q, 2H, $H_2C_{pyrrol.}$), 6.22 (s, 1H, $HC_{pyrrol.}$), 6.80 (A of AB_q, 2H, $J=16.0$ Hz, CH=), 6.94 (B of AB_q, 1H, CH=), 6.97 (m, 11H, $J=8.8$ Hz, $10\times H_{arom.}+$ CH=), 7.15–7.36 (m, 8H, $J=8.4$ Hz, $H_{arom.}$), 7.60 (s, 1H, $H_{arom.}$), 7.61–7.75 (m, 24H, $H_{arom.}$), 7.90 (d, 2H, $J=8.4$ Hz, $H_{arom.}$), 8.12–8.20 (m, 16H, $H_{arom.}$), 8.21 (s, 2H, $H_{arom.}$), 8.37 (t, 2H, $J=1.5$ Hz, $H_{arom.}$), 8.65 (t, 2H, $J=1.5$ Hz, $H_{arom.}$), 8.94 (t, 1H, $J=1.5$ Hz, $H_{arom.}$). ^{13}C NMR (50 MHz, $CDCl_3$): δ 165.54, 164.69, 164.61, 164.20, 163.90, 163.49, 163.06, 162.95, 162.80, 155.23, 152.68, 151.67, 151.43, 150.39, 150.12, 147.47, 146.26, 146.08, 146.00, 145.88, 145.76, 145.59, 145.43, 145.24, 145.11, 145.04, 144.72, 144.46, 144.35, 144.17, 143.95, 143.09, 142.62, 142.12, 141.92, 141.86, 141.67, 140.14, 139.52, 139.17, 137.76, 136.93, 136.85, 136.55, 135.20, 134.35, 132.58, 132.49, 132.28, 130.02, 128.72, 128.28, 127.62, 126.98, 123.59, 123.28, 121.17, 120.27, 118.87, 114.55, 111.00, 95.91, 82.89, 82.80, 70.09, 69.72, 69.52, 68.62, 68.52, 67.36, 67.18, 66.07, 65.79, 30.04, 29.80, 29.42, 28.98, 21.83. UV–vis λ_{max} (nm) (log ε, $CHCl_3$): 279 (5.31). IR (KBr) ν (cm^{-1}) 2223, 1726, 1598, 1055, 845, 538. MALDI-MS, *m/e* 3989.1 (M+1).

4.1.4. Synthesis of 2. Prepared as **1** from **6** (18.8 mg, 0.01 mmol). Dark brown solid. Quantitative yield. ^{1}H NMR (200 MHz, $CDCl_3$): δ 0.70–1.70 (m broad, 60H, $H_{aliph.}$), 1.71–2.0 (m broad, 20H, $5\times CO_2CH_2CH_2+5\times CH_2CH_2O$), 4.04 (t, 10H, $J=6.4$ Hz, CH_2O), 4.17 (s, 20H, C_5H_5), 4.37 (m, 18H, $8\times HCp+5\times CO_2CH_2$), 4.53 (t, 8H, $J=1.8$ Hz, HCp), 5.83 (AB_q, 2H, $H_2C_{pyrrol.}$), 6.25 (s, 1H, $HC_{pyrrol.}$), 6.76 (A of AB_q, 4H, $J=16.0$ Hz, CH=), 6.97 (m, 14H, $J=8.8$ Hz, $10\times H_{arom.}+4\times CH=$), 7.15–7.36 (m, 12H, $J=8.4$ Hz, $8\times H_{arom.}+4\times CH=$), 7.40 (s, 2H, $H_{arom.}$), 7.50 (s, 4H, $H_{arom.}$), 7.57–7.90 (m, 27H, $H_{arom.}$), 8.09–8.16 (m, 16H, $H_{arom.}$), 8.19 (s, 2H, $H_{arom.}$), 8.36 (t, 2H, $J=1.5$ Hz, $H_{arom.}$), 8.63 (t, 2H, $J=1.5$ Hz, $H_{arom.}$), 8.93 (t, 1H, $J=1.5$ Hz, $H_{arom.}$). ^{13}C NMR (50 MHz, $CDCl_3$): δ 165.08, 164.96, 164.59, 164.33, 163.93, 163.48, 163.30, 163.26, 160.65, 155.89, 153.99, 151.88, 151.84, 151.48, 150.82, 150.79, 150.63, 149.22, 148.42, 148.22, 148.01, 147.46, 147.25, 146.72, 146.63, 146.59, 146.57, 145.60, 145.26, 145.25, 145.11, 145.09, 144.77, 144.71, 144.54, 143.39, 143.28, 142.88, 144.21, 142.01, 141.74, 140.16, 137.11, 136.90, 133.46, 132.96, 132.84, 132.72, 132.54, 131.71, 131.40, 131.27, 130.73, 130.36, 130.21, 129.68, 128.51, 127.89, 127.16, 122.74, 121.54, 120.63, 118.99, 114.80, 114.62, 111.31, 81.01, 80.37, 70.70, 69.71, 68.58, 67.85, 66.07, 65.77, 53.57, 45.53, 29.89, 29.51, 29.42, 28.88, 28.58, 26.17, 22.87, 22.52. UV–vis λ_{max} (nm) (log ε, $CHCl_3$): 279 (5.37). IR (KBr) ν (cm^{-1}) 2218, 823, 533. MALDI-MS, *m/e* 4613.4 (M+1).

Acknowledgements

R.D. thanks the Swiss National Science Foundation (Grant no. 200020-103424) for financial support. This work was supported by the EU (RTN contract "FAMOUS", HPRN-CT-2002-00171), the Ministerio of Educación y Ciencia of Spain (Project CTQ2004-00364/BQU) and FEDER funds. L.P. thanks a grant from the Ministerio de Educación y Ciencia of Spain.

References and notes

1. Martín, N.; Sánchez, L.; Illescas, B.; Pérez, I. *Chem. Rev.* **1998**, *98*, 2527.
2. (a) Nierengarten, J.-F.; Eckert, J.-F.; Nicoud, J.-F.; Ouali, L.; Krasnikov, V.; Hadziioannou, G. *Chem. Commun.* **1999**, 617. (b) Eckert, J.-F.; Nicoud, J.-F.; Nierengarten, J.-F.; Liu, S.-G.; Echegoyen, L.; Barigelletti, F.; Armaroli, N.; Ouali, L.; Krasnikov, V.; Hadziioannou, G. *J. Am. Chem. Soc.* **2000**, *122*, 7467. (c) Peeters, E.; van Hal, P. A.; Knol, J.; Brabec, C. J.; Sariciftci, N. S.; Hummelen, J. C.; Janssen, R. A. J. *J. Phys. Chem. B* **2000**, *104*, 10174. (d) Marcos Ramos, A.; Rispens, M. T.; van Duren, J. K. J.; Hummelen, J. C.; Janssen, R. A. J. *J. Am. Chem. Soc.* **2001**, *123*, 6714. (e) Zerza, G.; Röthler, B.; Sariciftci, N. S.; Gómez, R.; Segura, J. L.; Martín, N. *J. Phys. Chem. B* **2001**, *105*, 4099. (f) Guldi, D. M.; Swartz, A.; Luo, C.; Gómez, R.; Segura, J. L.; Martín, N. *J. Am. Chem. Soc.* **2002**, *124*, 10875. (g) Martineau, C.; Blanchard, P.; Rondeau, D.; Delaunay, J.; Roncali, J. *Adv. Mater.* **2002**, *14*, 283.
3. (a) Imahori, H.; Sakata, Y. *Eur. J. Org. Chem.* **1999**, 2445. (b) Guldi, D. M. *Chem. Commun.* **2000**, 321. (c) Guldi, D. M. *Chem. Soc. Rev.* **2002**, *31*, 22.
4. (a) Guldi, D. M.; Maggini, M.; Scorrano, G.; Prato, M. *J. Am. Chem. Soc.* **1997**, *119*, 974. (b) Guldi, D. M.; Prato, M. *Acc. Chem. Res.* **2000**, *33*, 695.
5. (a) Yu, G.; Gao, J.; Hummelen, J. C.; Wudl, F.; Heeger, A. J. *Science* **1995**, *270*, 1789. (b) Brabec, C. J.; Sariciftci, N. S.; Hummelen, J. C. *Adv. Funct. Mater.* **2001**, *11*, 15. (c) Shaheen, S. E.; Brabec, C. J.; Sariciftci, N. S.; Padinger, F.; Fromherz, T.; Hummelen, J. C. *Appl. Phys. Lett.* **2001**, *78*, 841.
6. Hutchison, K.; Gao, J.; Schick, G.; Rubin, Y.; Wudl, F. *J. Am. Chem. Soc.* **1999**, *121*, 5611.

7. (a) Schmidt-Mende, L.; Fechtenkötter, A.; Müllen, K.; Moons, E.; Friend, R. H.; MacKenzie, J. D. *Science* **2001**, *293*, 1119. (b) Pisula, W.; Tomović, Ź.; El Hamaoui, B.; Watson, M. D.; Pakula, T.; Müllen, K. *Adv. Funct. Mater.* **2005**, *15*, 893.
8. (a) Deschenaux, R.; Even, M.; Guillon, D. *Chem. Commun.* **1998**, 537. (b) Even, M.; Heinrich, B.; Guillon, D.; Guldi, D. M.; Prato, M.; Deschenaux, R. *Chem. Eur. J.* **2001**, *7*, 2595. (c) Campidelli, S.; Vázquez, E.; Milic, D.; Prato, M.; Barberá, J.; Guldi, D. M.; Marcaccio, M.; Paolucci, D.; Paolucci, F.; Deschenaux, R. *J. Mater. Chem.* **2004**, *14*, 1266.
9. (a) Deschenaux, R.; Schweissguth, M.; Levelut, A.-M. *Chem. Commun.* **1996**, 1275. (b) Deschenaux, R.; Schweissguth, M.; Vilches, M.-T.; Levelut, A.-M.; Hautot, D.; Long, G. L.; Luneau, D. *Organometallics* **1999**, *18*, 5553.
10. Ruiz, J.; Pradet, C.; Varret, F.; Astruc, D. *Chem. Commun.* **2002**, 1108.
11. (a) Valério, C.; Fillaut, J.-L.; Ruiz, J.; Guittard, J.; Blais, J.-C.; Astruc, D. *J. Am. Chem. Soc.* **1997**, *119*, 2588. (b) Casado, C. M.; González, B.; Cuadrado, I.; Alonso, B.; Morán, M.; Losada, J. *Angew. Chem., Int. Ed.* **2000**, *39*, 2135. (c) Alonso, B.; Casado, C. M.; Cuadrado, I.; Morán, M.; Kaifer, A. E. *Chem. Commun.* **2002**, 1778. (d) Daniel, M.-C.; Ba, F.; Ruiz Aranzaes, J.; Astruc, D. *Inorg. Chem.* **2004**, *43*, 8649.
12. (a) Prato, M.; Maggini, M. *Acc. Chem. Res.* **1998**, *31*, 519. (b) Tagmatarchis, N.; Prato, M. *Synlett* **2003**, 768.
13. Chuard, T.; Deschenaux, R. *J. Mater. Chem.* **2002**, *12*, 1944.
14. Bracher, P. J.; Schuster, D. I. In *Fullerenes: From Synthesis to Optoelectronic Properties*; Guldi, D. M., Martín, N., Eds.; Kluwer Academic, 2002; pp 163–212.
15. Gust, D.; Moore, T. A.; Moore, A. L. *Acc. Chem. Res.* **2001**, *34*, 40.
16. A residual absorption of light by the ferrocene dendrimer cannot be excluded.
17. (a) D'Souza, F.; Zandler, M. E.; Smith, P. M.; Deviprasad, G. R.; Arkady, K.; Fujitsuka, M.; Ito, O. *J. Phys. Chem. A* **2002**, *106*, 649. (b) Zandler, M. E.; Smith, P. M.; Fujitsuka, M.; Ito, O.; D'Souza, F. *J. Org. Chem.* **2002**, *67*, 9122.